

**KINETIC-ALFVEN-WAVE CURRENT DRIVE
IN PLASMAS
WITH ELONGATED CROSS SECTIONS**

Satish Puri and Rolf Wilhelm

IPP 4/236

ABSTRACT

September 1988



MAX-PLANCK-INSTITUT FÜR PLASMAPHYSIK

8046 GARCHING BEI MÜNCHEN

MAX-PLANCK-INSTITUT FÜR PLASMAPHYSIK
GARCHING BEI MÜNCHEN

**KINETIC-ALFVEN-WAVE CURRENT DRIVE
IN PLASMAS
WITH ELONGATED CROSS SECTIONS**

Satish Puri and Rolf Wilhelm

IPP 4/236

September 1988

Die nachstehende Arbeit wurde im Rahmen des Vertrages zwischen dem Max-Planck-Institut für Plasmaphysik und der Europäischen Atomgemeinschaft über die Zusammenarbeit auf dem Gebiete der Plasmaphysik durchgeführt.

Kinetic-Alfven-Wave Current Drive in Plasmas with Elongated Cross Sections

S. Puri and R. Wilhelm

Max-Planck Institut für Plasmaphysik, EURATOM Association,
Garching bei München, Federal Republic of Germany

ABSTRACT

Proper optimization of antenna parameters can lead to high efficiency ($Rn_{20}I/P \gtrsim 3$) kinetic-Alfven-wave current drive in plasmas with elongated cross sections. The optimal parameters include (i) finite, non-zero azimuthal wave number $m = 1$, (ii) large toroidal wave number $n = 5 - 8$, (iii) an antenna array consisting of at least n elements with adjacent elements phased $\pi/2$ apart, (iv) Faraday shielding, and (v) plasma cross-section elongation $s > 1.5$, which together with the finite β , helps in moderating the trapped-particle effects by locating the resonance close to the plasma axis.

PACS numbers: 52.50.Gj; 52.40.Db; 52.55.Fa

Non-inductive current drive for attaining steady-state operation is a significant feature of the future Tokamak devices such as NET and ITER. However, the poor current-drive efficiency ($\gamma = Rn_{20}I/P \lesssim 0.4$) of the schemes presently under consideration limits the fusion power gain to $P_{fusion}/P_{auxiliary} \sim 5$, which is an order of magnitude lower than the requirements of an economic fusion reactor.¹

Wort² has suggested the use of subthermal (parallel phase velocity, v_p less than the electron thermal velocity, v_t) waves for obtaining higher current-drive efficiencies. Subthermal waves have the advantage of transferring a high parallel momentum content to the electrons^{2,3}; but the current-drive efficiency might be severely curtailed by the high collisional losses and trapped-particle effects⁴. The subthermal current-drive scheme using the kinetic Alfvén wave⁵⁻⁷ (KIN) is further hampered by poor coupling efficiency (due to inadequate wave conversion³) as well as by limited penetration⁸⁻¹⁰ into the plasma core.

In this Letter we show that the problems encountered in the KIN current-drive scheme can be successfully resolved. Through a judicious choice of the antenna parameters, it would be possible to attain high current-drive efficiencies ($\gamma \gtrsim 3$) in hot, reactor-grade plasmas with elongated cross sections using the subthermal KIN at frequencies around 1 MHz.

Figure 1 shows the qualitative Alfvén-wave dispersion characteristics in a slab geometry for $k_y = 0$.⁸ The plasma density and temperature are assumed to increase along x and the magnetic field is in the z direction. ϵ_x , ϵ_y and ϵ_z are the components of the dielectric tensor ϵ , $\mathbf{n} = \mathbf{k}/k_0$, and $\epsilon_{L,R} = \epsilon_x \pm i\epsilon_y$. The propagating cold-plasma torsional Alfvén wave (TOR) becomes the evanescent hot-plasma KIN at $\zeta = v_p/v_t \approx 1$ which typically occurs close to the plasma edge for $T_e \sim 100$ eV. Near the Alfvén layer at $\epsilon_x = n_z^2$, KIN assumes a propagating character and is subject to strong Landau damping.⁶ Direct coupling to the propagating branch of KIN by tunneling through the evanescent KIN to the left of the Alfvén layer is precluded by the strong evanescence. The Alfvén resonance $\epsilon_x = n_z^2$ may, however, be approached via coupling to the weakly

evanescent compressional Alfvén wave (COM).⁵⁻⁷ Near the Alfvén layer, the evanescent COM launched by the antenna partly couples to the propagating COM in the plasma interior and partly converts to the propagating KIN via the process of wave conversion.⁶ The energy coupled to KIN is readily assimilated through electron Landau damping giving rise to plasma heating and current drive.^{6,7}

The success of this scheme is critically dependent upon two factors, namely, (i) the launching of COM with a minimum of evanescence between the antenna and the Alfvén layer, and (ii) efficient wave conversion from COM to KIN near the Alfvén layer. These happen to be contradictory requirements: The first is best satisfied at low values of m and n , while the second demands the choice of finite $m = 1$, and large $n = 5 - 8$ values.⁸⁻¹⁰

For the $k_y = 0$ case, the evanescent COM launched by the antenna predominantly couples to the propagating COM in the plasma interior with a correspondingly low wave conversion efficiency to KIN.³ The introduction of a finite k_y translates the axis uniformly upwards by the amount k_y^2 in Fig.1, thereby curtailing the propagation region of COM in the plasma interior and forcing a larger fraction of the antenna power into the propagating branch of KIN. In Fig.8 of Ref.10, although the $m = 1$ COM component launched by the antenna is less than a quarter of the $m = 0$ component for the extant antenna parameters, the energy coupled to the $m = 1$ modes exceeds that of the $m = 0$ mode by a factor of fifty; i.e., the coupling efficiency of the $m = 1$ case is over two orders of magnitude superior compared to the $m = 0$ case. A similarly dramatic improvement in the antenna loading with an increasing toroidal number is exhibited in Fig.1 of Ref.10. An approximate analytical explanation of this behavior is provided in the Appendix of Ref.10.

The requirement of a finite azimuthal wave number $m = 1$ and a large toroidal wave number $n = 5 - 8$ imposes the serious penalty of limited radial access of the antenna energy into the plasma due to the increased evanescence experienced by COM. Acceptable antenna coupling ($Q \sim 15$) is feasible only for the resonance layer location

$r_0 > 0.67a$, corresponding to a penetration depth $p = 0.33a + d$, where a is the plasma radius and d is the antenna-plasma separation.^{9,10} Current drive confined to the outer one-third plasma radius would be undesirable both on account of low current-drive efficiency (limited by collisions and trapped-particle effects) and poor confinement. The present trend towards elongated plasma cross-sections together with the shift in the plasma axis due to finite β effects in reactor-grade plasmas radically improves this dismal outlook.

For the elliptical plasma cross-section of elongation s (Fig.2), the antenna radius is given by

$$r_A \approx (a + d)s^2 . \quad (1)$$

The increase in the antenna radius leads to a reduction in the wave evanescence. Since the penetration depth p is considerably less than the antenna radius, a reasonable estimate of p is possible using the slab approximation corrected for the cylindrical geometry. Let $k_y = \tilde{r}^{-1}$ and $k_z = n(R + r)^{-1}$, where $\tilde{r} = r_A - (a + d) + r$ and R is the plasma major radius. The wave evanescence causes a steady decrease of the wave amplitude as we move away from the antenna. The energy density at the resonance position r_0 , relative to its value at the antenna surface is $G = \exp(-\Gamma)$, where

$$\Gamma = 2ia \int_{\rho_0}^{1+\rho_d} k_x(\rho) d\rho , \quad (2)$$

$\rho = r/a$, $\rho_0 = r_0/a$, $\rho_d = d/a$, k_x is given by the approximate COM dispersion relation

$$k_x^2 = k_0^2 \epsilon_x - k_y^2 - k_z^2 , \quad (3)$$

and $\epsilon_x = 1 + (n_z^2 - 1)(1 - \rho^2)/(1 - \rho_0^2)$ for a parabolic density profile. G is plotted as a function of ρ_0 and s for $n = 6$ in Fig.3, assuming $A = R/a = 4$, $\rho_d = 0.1$, and $n_z^2 \gg 1$. As s increases from 1 to 2, ρ_0 can be lowered from 0.67 to 0.37 keeping the antenna coupling unchanged. Since the elongated plasmas tend to be D -shaped rather than elliptical, r_A given by Eq.(1) is an overestimate. However, Fig.3 shows that the resultant error from this overestimate is small because the improvement in coupling tapers off with increasing s .

Further enhancement in the penetration of antenna energy into the plasma interior is contributed by the finite β in reactor-grade plasmas. Finite β is accompanied by an outward shift of the plasma axis which for the reactor parameters may amount to as much as a quarter of the plasma radius. Thus, it would be possible to locate the resonant layer at $r_0 \sim 0.2a$; a considerable improvement over the existing assessment.

The Alfvén-wave resonance relation $\omega = (nc/R)(\omega_{ci}/\omega_{pi})$, allows one to locate the position of the resonant layer through the choice of ω . By selecting several different frequencies to drive the antennas simultaneously, it would be possible to obtain arbitrary plasma current profiles, subject to the condition $r_0(\omega) \geq 0.2a$. Deployment of $4n$ antennas uniformly around the torus circumference with adjacent sections phased $\pi/2$ apart would exclude the presence of unwanted resonances between the resonant layer and the plasma edge. Usage of fewer antennas would be accompanied by unwanted toroidal harmonics; the low- n components being particularly undesirable as they give rise to absorption near the edge. Fortunately, the sharp decrease in the coupling efficiency at low- n values tends to limit the damage.^{9,10}

The antenna efficiency $\eta_A = P_P/P_A$, where P_P is the power coupled into the plasma and P_A is the power entering the antenna terminals (the remainder represents ohmic losses in the antenna, the wall, and the Faraday shield), for coupling to KIN is typically over 99%; i.e., P_P is substantially the same as P_A .^{9,10}

The current density induced in the plasma is related to the power density by

$$j(r) \approx \frac{e}{m} \frac{P(r)}{\tilde{\nu}_{ei}(r)v_A(r)}, \quad (4)$$

where v_A is the local Alfvén speed, and $\tilde{\nu}_{ei} = \nu_{ei}[1 - (\rho/A)^{1/2}]^{-2}$ is the Spitzer collision frequency corrected for the trapped-particle effects. The current-drive efficiency becomes

$$\gamma = \frac{\langle n_{20} \rangle RI}{P_P} = \frac{\langle n_{20} \rangle}{2\pi} \frac{e}{m} \frac{\int_0^1 \tilde{\nu}_{ei}^{-1}(\rho)v_A^{-1}(\rho)P(\rho)\rho d\rho}{\int_0^1 P(\rho)\rho d\rho}, \quad (5)$$

where $\langle n_{20} \rangle \times 10^{20} m^{-3}$ is the volume-averaged plasma density. Assuming $n_e(\rho) =$

$n_{e0}(1 - \rho^2)^{\chi_n}$ and $T_e(\rho) = T_{e0}(1 - \rho^2)^{\chi_T}$ yields

$$\gamma = \frac{13.5\mu^{1/2} \langle \beta \rangle^{1/2} \langle T_{keV} \rangle}{Z \langle \ln \Lambda \rangle} \frac{\chi_T + 1}{\chi_n + 1} (\chi_n + \chi_T + 1)^{1/2} \mathfrak{S}, \quad (6)$$

where μ is the atomic mass number, $\langle \beta \rangle$ is the volume-averaged toroidal β , $\langle T_{keV} \rangle$ is the volume-averaged electron temperature in keV , and $\langle \ln \Lambda \rangle$ is the weighted Coulomb logarithm. The profile and trapped-particle effects are contained in

$$\mathfrak{S} = \frac{\int_0^1 (1 - \rho^2)^\alpha \left[1 - (\rho/A)^{1/2}\right]^2 P(\rho) \rho d\rho}{\int_0^1 P(\rho) \rho d\rho}, \quad (7)$$

where, $\alpha = 1.5\chi_T - 0.5\chi_n$.

KIN has a radial damping length of $\sim 1 cm$.¹¹ Displacement of the resonant surface with respect to the magnetic surface, radial current diffusion, as well as plateau formation in the electron-velocity-distribution function would further boost the radial extent of the absorption region. Nevertheless, for an approximate evaluation of \mathfrak{S} in Eq.(7), we assume that the power is absorbed at discrete radial locations ρ_l , so that

$$\mathfrak{S} \approx \frac{\sum_{l=1}^L F(\rho_l, \alpha, A) P(\rho_l) \rho_l}{\sum_{l=1}^L P(\rho_l) \rho_l}, \quad (8)$$

where

$$F(\rho, \alpha, A) = (1 - \rho^2)^\alpha \left[1 - (\rho/A)^{1/2}\right]^2. \quad (9)$$

Figure 4 is a plot of $F(\rho, \alpha, A)$ as a function of ρ and α for $A = 4$. The $\alpha = 0$ curve shows the trapped-particle effect on $F(\rho, \alpha, A)$. For the ideal case (using $4n$ antennas) of a single resonance occurring at ρ_0 , $\mathfrak{S} \equiv F(\rho_0, \alpha, A)$. Assuming $\rho_0 = 0.25$, $\chi_n = 1$ and $\chi_T = 1.5$, one obtains from Fig.4, $F(0.25, 1.75, 4) \approx 0.5$. For $\mu = 2.5$, $\langle \beta \rangle = 0.05$, $\langle T_{keV} \rangle = 15$, $Z = 1.5$, and $\langle \ln \Lambda \rangle = 17$, $\gamma \approx 3.3$. Usage of fewer antennas would divert part of the coupled power to larger radii resulting in diminished values of γ . For the case of coupling with n antennas located in one torus quadrant, $\gamma \sim 3$. The current-drive efficiency γ is almost an order of magnitude higher than the alternative

approaches such as lower-hybrid resonance or transit-time magnetic pumping. Moreover, for realistic parameters ($n_e \sim 2 \times 10^{20} m^{-3}$, $m \neq 0$), the lower-hybrid and TTMP current drive will be peaked near the plasma surface, whereas the KIN approach permits an almost arbitrary tailoring of the current profile. Further improvements in the current-drive efficiency may accrue from (i) local-temperature increase, (ii) recovery of the canonical angular momentum via particle detrapping³, and (iii) bootstrap current⁴.

The principal objective of this communication is to demonstrate the effectiveness of kinetic-Alfven-wave current drive in *elongated-cross-section plasmas using optimized antenna parameters*. The pessimistic appraisal of Ref.3 regarding the wave-conversion efficiency from COM to KIN can be reversed by using a finite azimuthal wave number, $m = 1$.⁸ The finite m , however, limits the access into the plasma core due to fundamental Bessel function properties. The penetration problem is further accentuated by the requirement of a large toroidal wave number ($n = 5 - 8$) necessary for optimal coupling.^{9,10} We have shown that for the case of hot, elongated-cross-section plasmas ($s > 1.5$), access to the plasma core is made possible by the reduction in the *relative* (compared with the antenna radius) penetration distance entailed. Localization of current drive close to the plasma axis alleviates the problems due to the trapped-particle effects. Finally, proper shielding using a Faraday screen that blocks the parallel-electric-field component emanating from the antenna sides¹² would avert plasma production and associated density-rise¹³. We conclude that the kinetic-Alfven-wave current drive is a highly credible proposition and merits serious consideration.

References

1. R. Wilhelm, in *Proc. 15th Symp. on Fusion Tech.*, Utrecht, 1988, (CEC, Pergamon Press), to be published.
2. D. J. H. Wort, *Plasma Phys.* **13**, 258 (1971).
3. N. J. Fisch and C. F. F. Karney, *Phys. Fluids* **24**, 27 (1981).
4. R. J. Bickerton, *Comments Plasma Phys. Controlled Fusion* **1**, 95 (1972).
5. W. Grossman and J. A. Tataronis, *Z. Phys.* **261**, 217 (1973).
6. A. Hasegawa and L. Chen, *Phys. Rev. Lett.* **32**, 454 (1974).
7. A. Hasegawa, *Nuclear Fusion* **20**, 1158 (1980).
8. D. W. Ross, G. L. Chen and S. M. Mahajan, *Phys. Fluids* **25**, 652 (1982).
9. S. Puri, *Nucl. Fusion* **27**, 229 (1987).
10. S. Puri, *Nucl. Fusion* **27**, 1091 (1987).
11. S. Puri, in *Proc. 8th Int. IAEA Conf.*, Brussels, 1980 (IAEA, Vienna **2**, 51, 1981).
12. S. Puri, in *Proc. 15th Eur. Conf. on Controlled Fusion and Plasma Heating*, Dubrovnik, 1988 (EPS, Brussels **12B**, Part III, 952, 1988).
13. G. A. Collins *et al.*, *Phys. Fluids* **29**, 2260 (1986).

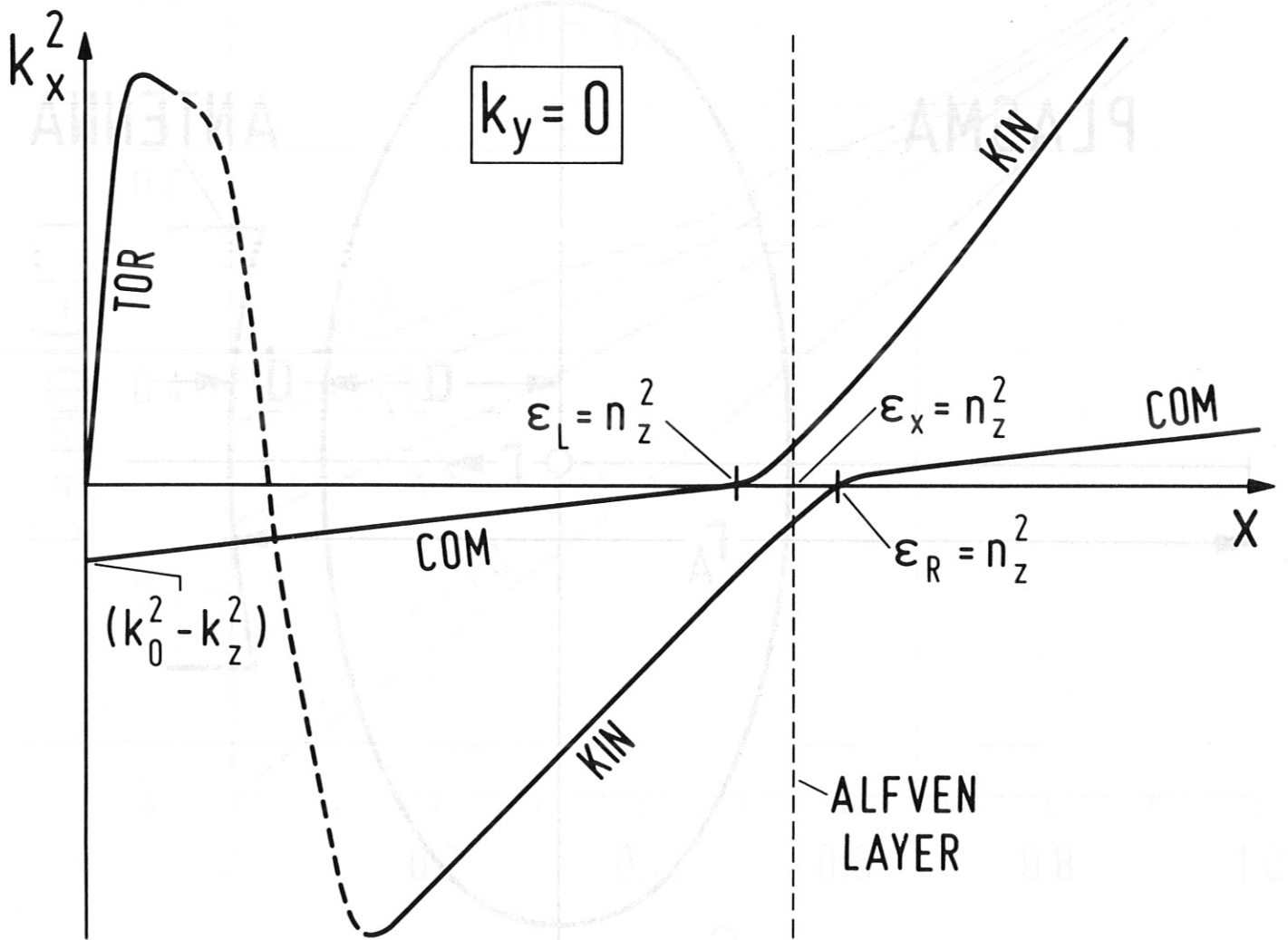


Fig.1 Qualitative Alfvén wave dispersion characteristics.

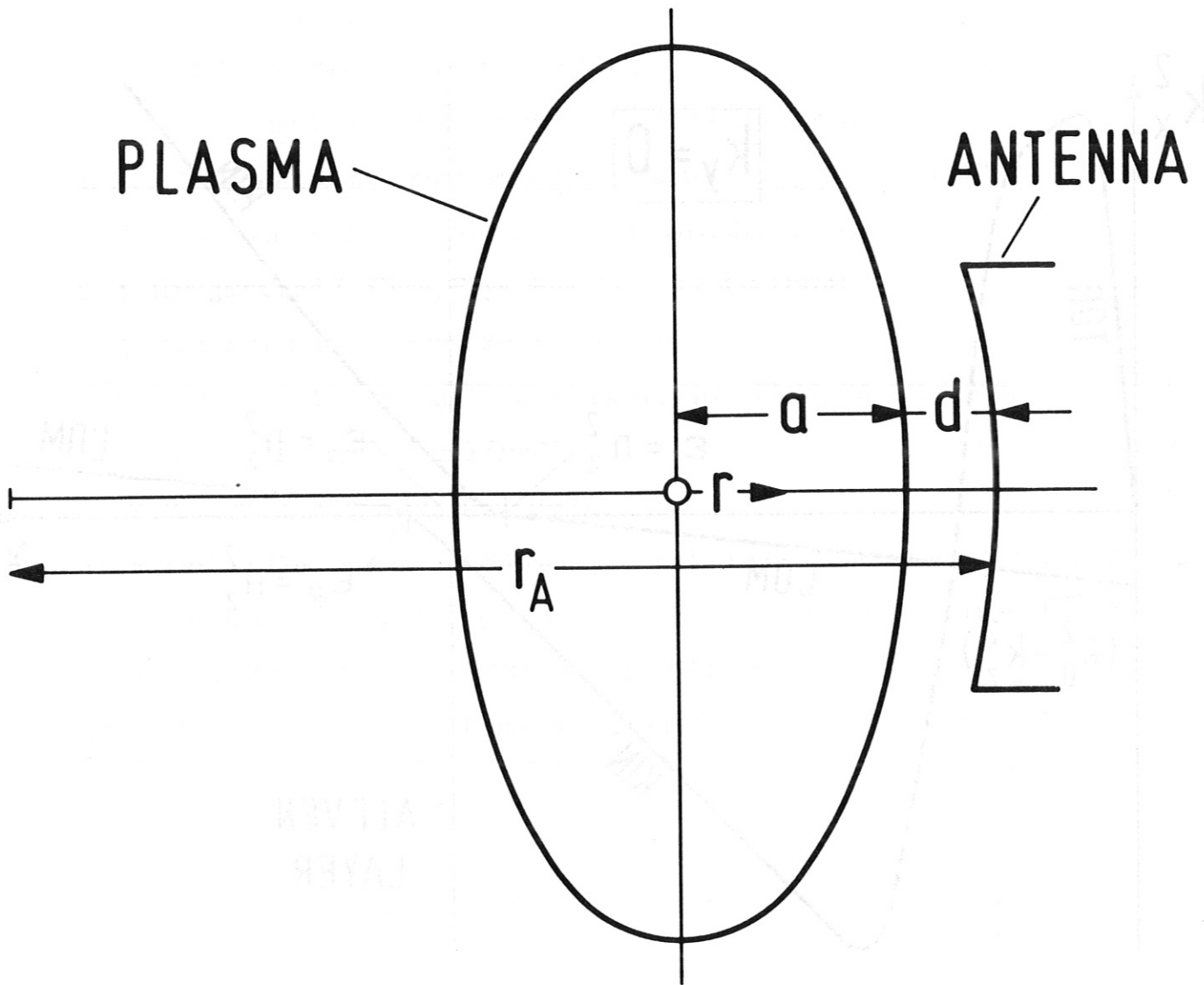


Fig.2 Elongated-cross-section plasma geometry.

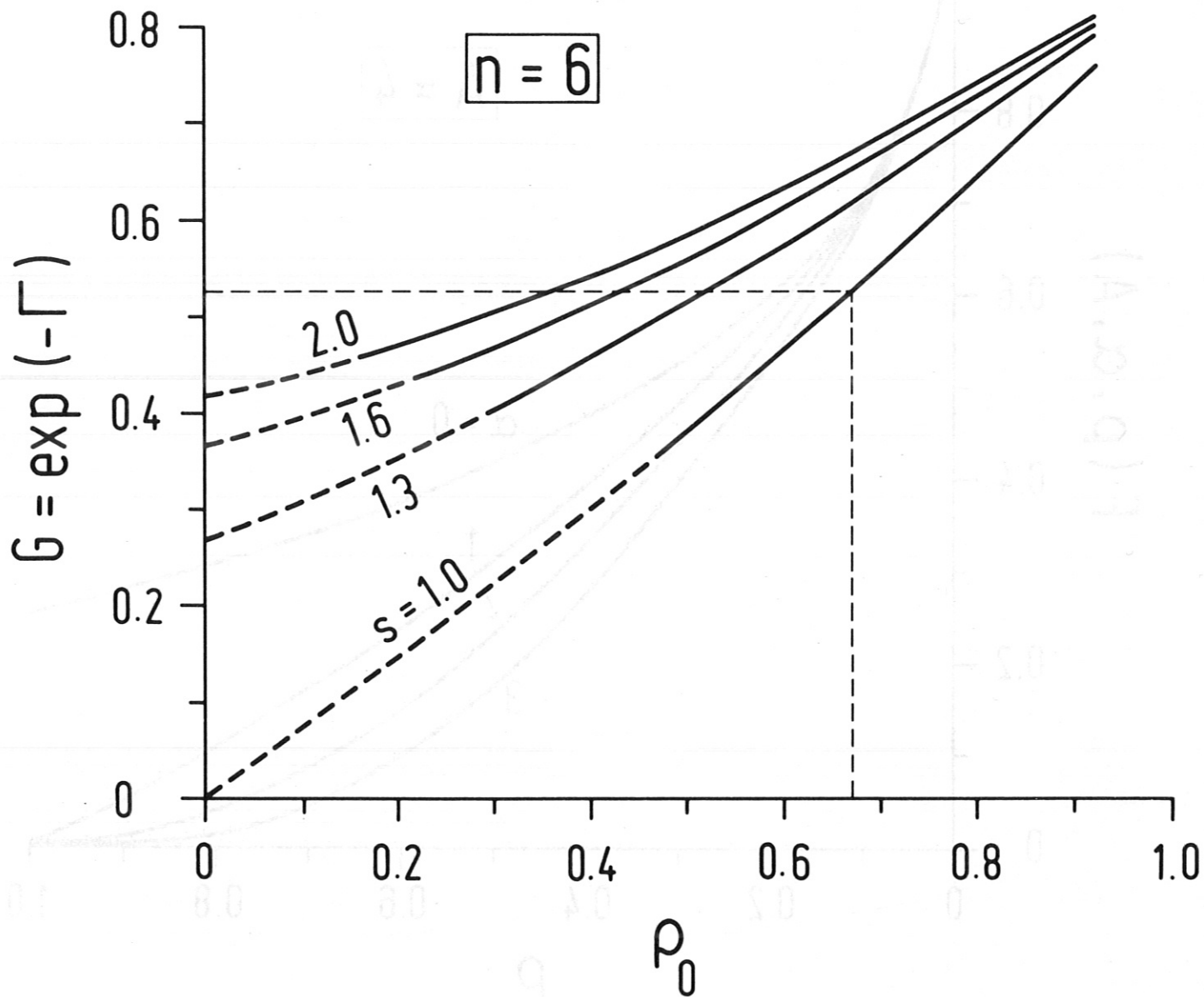


Fig.3 Relative energy density $G = \exp(-\Gamma)$ versus the resonance location.

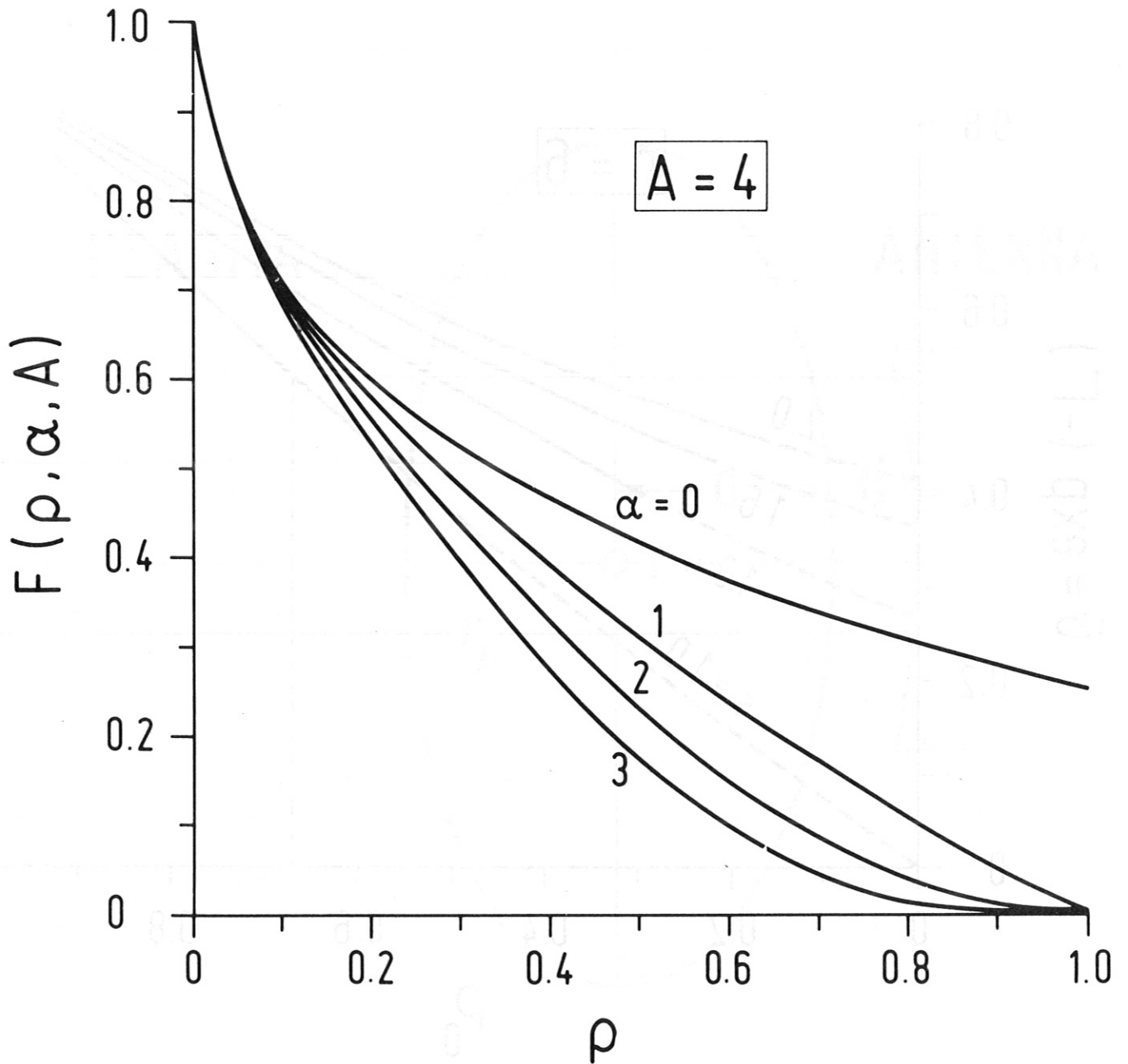


Fig.4 Function $F(\rho, \alpha, A)$ showing the effect of the resonance location on the current-drive efficiency.